

## CFD Studies of Combustion in Direct Injection Single Cylinder Diesel Engine Using Non-Premixed Combustion Model

S Gavudhama Karunanidhi\*, Nithin Balakrishnan\*\*, G Subba Rao\*\*\*

Assoc.Profesor\*( Department of Mechanical Engg MES College of Engg Kuttipuram, Kerala)

PG Scholar, \*\* (MES College of Engineering, Kuttippuram,Kerala, Calicut University)

Principal, \*\*\* (Geethanjali Institute of Science and Technology, Nellore)

### ABSTRACT

In this study the simulation process of non-premixed combustion in a direct injection single cylinder diesel engine has been described. Direct injection diesel engines are used both in heavy duty vehicles and light duty vehicles. The fuel is injected directly into the combustion chamber. The fuel mixes with the high pressure air in the combustion chamber and combustion occurs. Due to the non-premixed nature of the combustion occurring in such engines, non-premixed combustion model of ANSYS FLUENT 14.5 can be used to simulate the combustion process. A 4-stroke diesel engine corresponds to one fuel injector hole without considering valves was modeled and combustion simulation process was studied. Here two types of combustion chambers were compared. Combustion studies of both chambers:- shallow depth and hemispherical combustion chambers were carried out. Emission characteristics of both combustion chambers had also been carried out. The obtained results are compared. It has been found that hemispherical combustion chamber is more efficient as it produces higher pressure and temperature compared to that of shallow depth combustion chamber. As the temperature increases the formation of  $\text{NO}_x$  emissions and soot formation also get increased.

**Keywords**– CFD, Combustion modeling, Diesel combustion, k- $\epsilon$  model,  $\text{NO}_x$  emissions

### I. INTRODUCTION

In direct injection diesel engines there are different types of combustion chambers. Each one is having different characteristics of producing pressure, temperature and emissions. Here a detailed study has been carried out between two combustion chambers in order to have a clear clarification in studying the change in pressure temperature and emission characteristics. Two combustion chambers:- shallow depth chamber (SCC) and hemispherical combustion chamber (HCC) were taken into consideration. The two combustion chambers were modeled (a sector geometry of  $60^\circ$  using ANSYS WORKBENCH and analysis part were carried out using CFD tool (Fluent, ANSYS 14.5 package). By using the finite volume method the design and analysis of combustion chambers, emission characteristic study were done for both combustion chambers. Proper comparison of the results were carried and percentage rise in pressure and temperature had been calculated. Carnot efficiency of both of the combustion chambers were calculated and had found out which one is more efficient.

### II. PROCEDURE IN COMPUTATION

The combustion simulation of compression ignition engine with different piston configurations were developed using Fluent software (ANSYS 14.5 package) and the various equations of the multi-

dimensional model were solved by the software automatically. The main inputs include engine speed, injection details of single injection, bore, stroke, connecting rod length, initial pressure and temperature[1].The program concerning the simulation model predicts the cylinder pressure, cylinder temperature, emission etc. The results including graphs and various contours (pressure, temperature,  $\text{NO}_x$  and Soot) were generated by Fluent software.

### III. DEFINITION OF MODEL

Two 3D cylinder geometries with centrally located injector were considered. The mesh was created using ANSYS WORKBENCH. The engine geometry details and specification details are given below. A hex dominant mesh was created uniformly throughout the area and analyzed using FLUENT, ANSYS 14.5 package. The complete meshed geometry contains 18644 faces and 42932 nodes.

Fig.1 Shows the meshed geometry of the cylinder.

Connecting rod length :140 mm

Bore :80 mm

Crank radius :55 mm

Crank shaft speed :1500 rpm

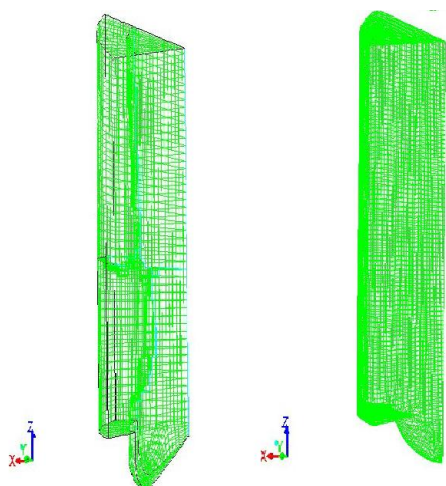


Fig.1 Meshed Geometries of the cylinder.

#### IV. MODELING TURBULENCE

Turbulent flows are characterized by fluctuating velocity fields. These fluctuations mix transported quantities such as momentum, energy, and species concentration, and cause the transported quantities to fluctuate as well. Since these fluctuations can be of small scale and high frequency, they are too computationally expensive to simulate directly in practical engineering calculations. Instead, the instantaneous (exact) governing equations can be time-averaged or otherwise manipulated to remove the small scales, resulting in a modified set of equations that are computationally less expensive to solve. However, the modified equations contain additional unknown variables, and turbulence models are needed to determine these variables in terms of known quantities. In this analysis standard k-ε model[1] is used.. In the derivation of the k- ε model, the assumption is that the flow is fully turbulent, and the effects of molecular viscosity are negligible. The standard k-ε model is therefore valid only for fully turbulent flows. The turbulent (or eddy) viscosity,  $\mu_t$ , is computed by combining  $k$  and  $\epsilon$  as follows:

$$\mu_t = \rho C_\mu \frac{k^2}{\epsilon}$$

#### V. BOUNDARY CONDITIONS

The boundary conditions should be given after modeling the geometry .In the analysis viscous standard k-e model is enabled for non premixed combustion model. The injection parameters and specifications are given below

- X-position :0.50038 mm
- Y- velocity :468 m/s
- Diameter :0.287 mm
- Temperature :341 K
- Flow rate :0.001044 kg/S
- Start crank angle :355 deg

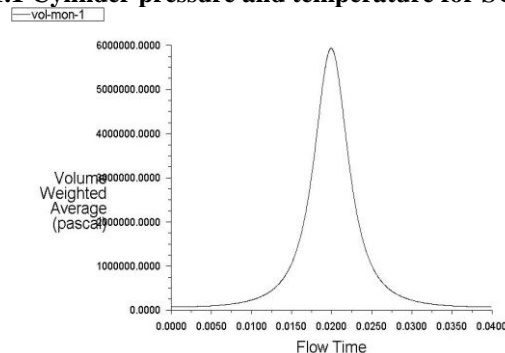
Stop crank angle :377deg

### VI. RESULTS AND DISCUSSIONS

#### 1. Combustion characteristics for SCC

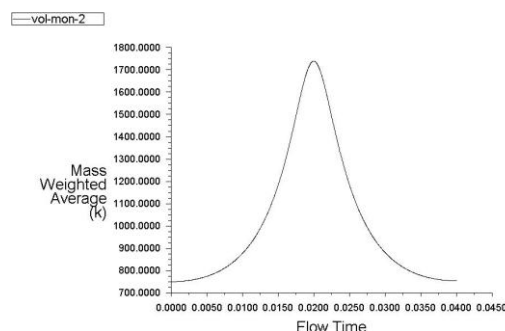
The combustion characteristics for both shallow depth and hemispherical combustion chambers are done..And the values of peak pressure and the temperature was approximately equal to the theoretical values.

##### 1.1 Cylinder pressure and temperature for SCC



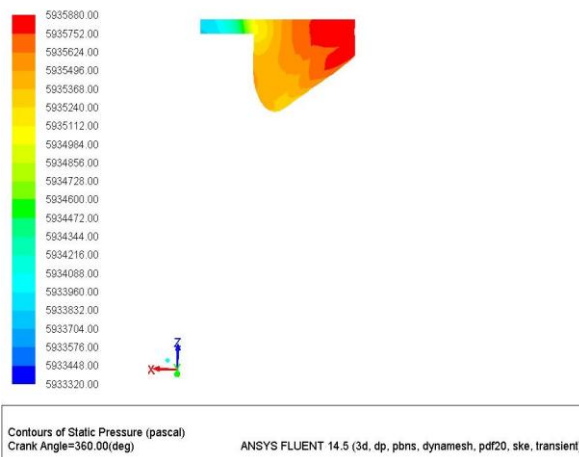
Convergence history of Static Pressure on fluid  
 Crank Angle=540.00(deg) ANSYS FLUENT 14.5 (3d, dp, pbns, dynamesh, pdf20, ske, transient)

Fig. 2. Pressure v/s Flow time



Convergence history of Static Temperature on fluid  
 Crank Angle=540.00(deg) ANSYS FLUENT 14.5 (3d, dp, pbns, dynamesh, pdf20, ske, transient)

Fig. 3. Temperature v/s Flow time



Contours of Static Pressure (pascal)  
 Crank Angle=360.00(deg) ANSYS FLUENT 14.5 (3d, dp, pbns, dynamesh, pdf20, ske, transient)

Fig 4. Contours of static pressure at 360° CA

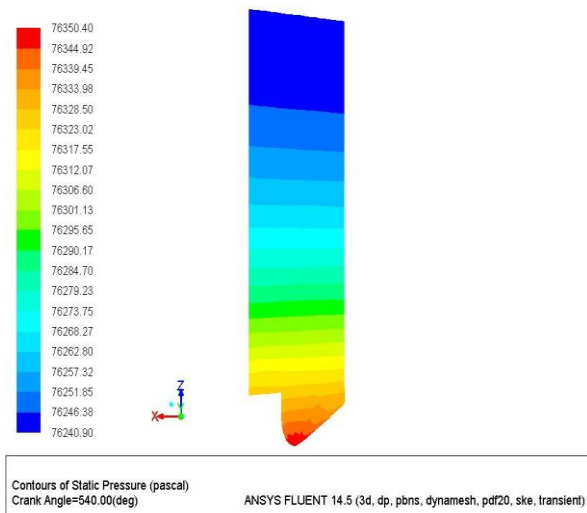


Fig 5. Contours of static pressure at 540<sup>0</sup> CA

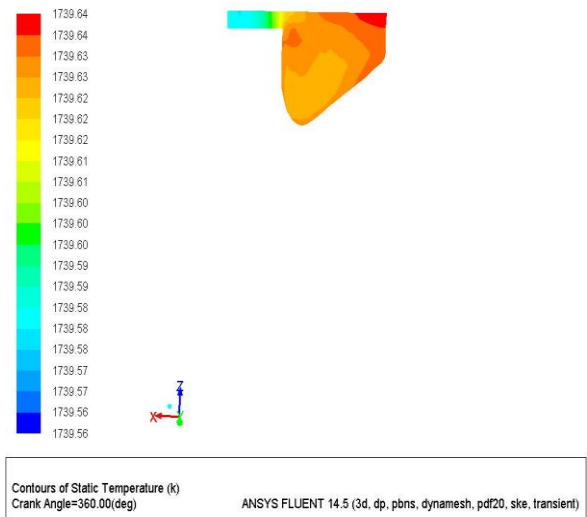


Fig 6. Contours of static temperature at 360<sup>0</sup> CA

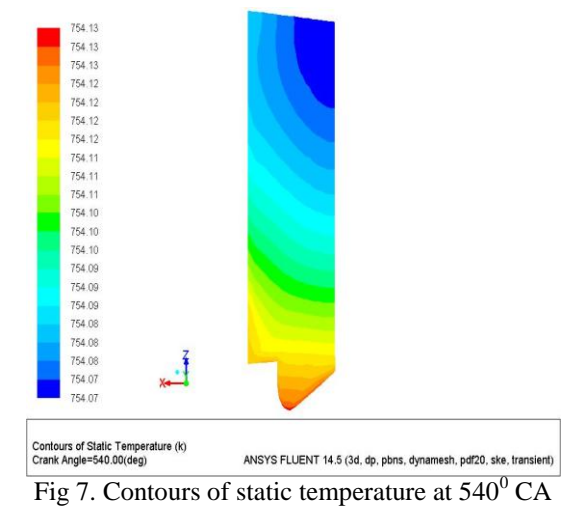


Fig 7. Contours of static temperature at 540<sup>0</sup> CA

From the above graphs and contours at crank angles 360<sup>0</sup> and 540<sup>0</sup>, it has been observed that the

peak cylinder pressure is about  $59.34 \times 10^5$  Pa and cylinder peak temperature of about 1739.56 K.

### 1.2 Emission characteristics for SCC

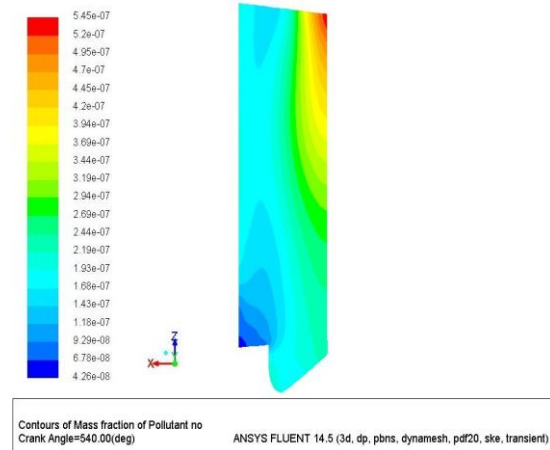


Fig 8. Contours of mass fraction of pollutant NO

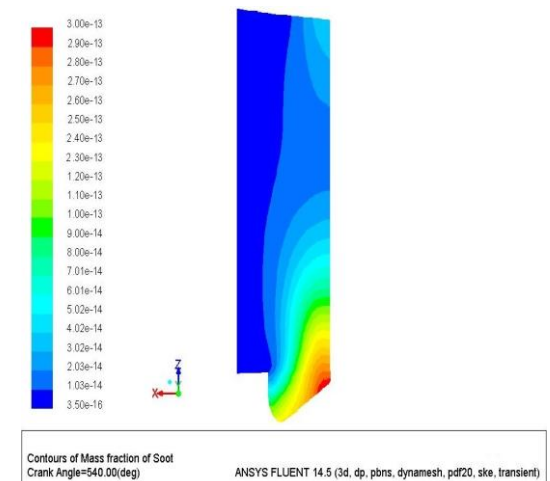


Fig 9. Contours of mass fraction of soot

From the contours of mass fraction of NO<sub>x</sub> emissions and soot formation it has been understood that NO<sub>x</sub> formation is occurring at regions where the temperature is high and soot formation, at regions where temperature is comparatively low.

## 2. Combustion characteristics for HCC

### 2.1 Cylinder pressure and temperature for HCC

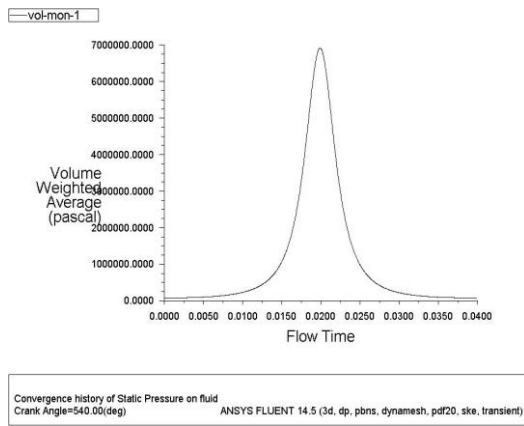


Fig. 10. Pressure v/s Flow time

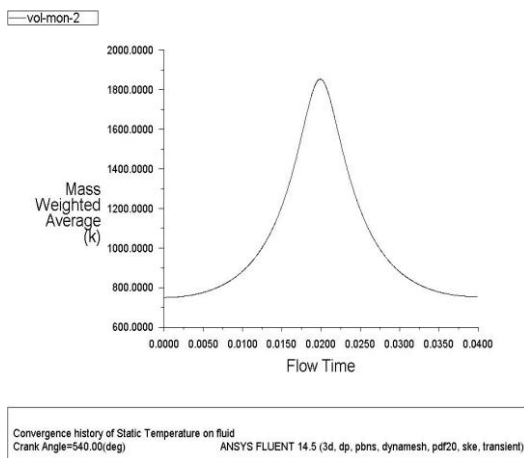


Fig. 11. Temperature v/s Flow time

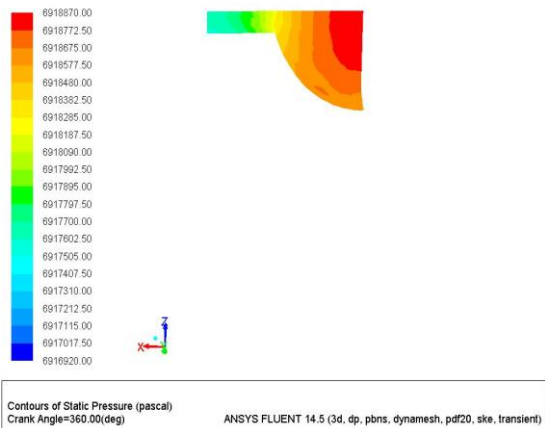


Fig. 12. Contours of static pressure at 360<sup>0</sup> CA

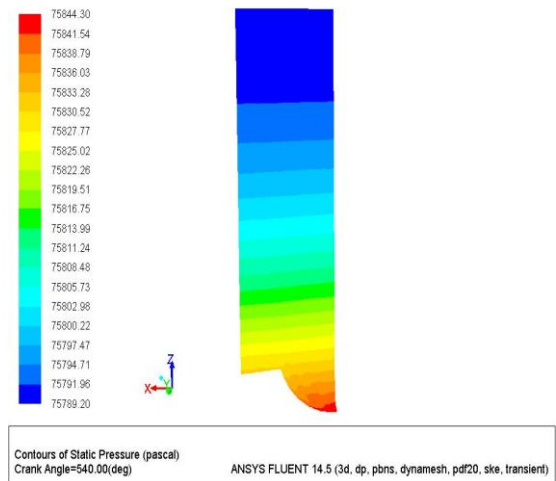


Fig. 13. Contours of static pressure at 540<sup>0</sup> CA

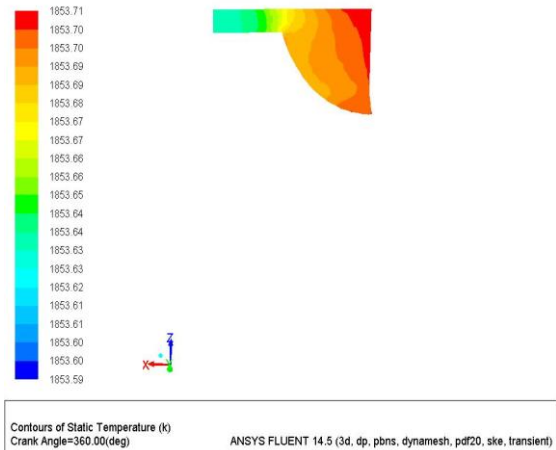


Fig. 14. Contours of static temperature at 360<sup>0</sup> CA

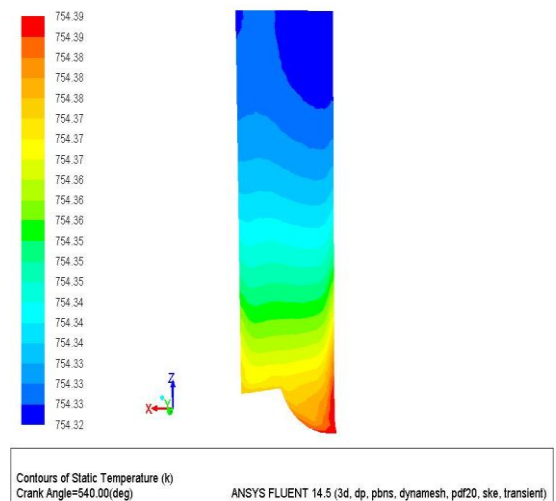


Fig. 15. Contours of static temperature at 540<sup>0</sup> CA

From the above graphs and contours at crank angles 360<sup>0</sup> and 540<sup>0</sup>, it has been observed that the

peak cylinder pressure is about  $69.19 \times 10^5$  Pa and cylinder peak temperature of about 1853.71 K.

### 2.2 Emission characteristics for HCC

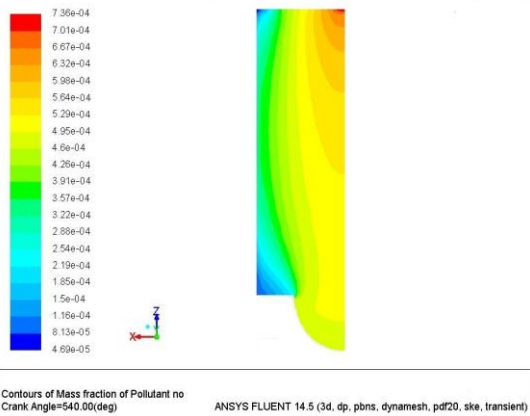


Fig 14. Contours of mass fraction of pollutant NO

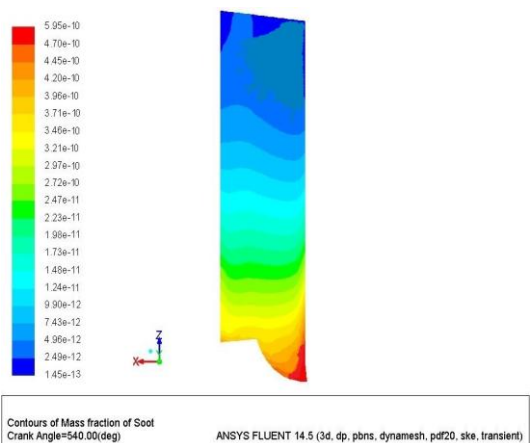


Fig 15. Contours of mass fraction of soot

From the contours of mass fraction of  $\text{NO}_x$  emissions and soot formation it has been understood that  $\text{NO}_x$  formation is occurring at regions where the temperature is high and soot formation, at regions where temperature is comparatively low.

### 3. Comparison of results

Table 1. Result comparison

Combustion chamber	Static Pressure (Pa)	Static temperature(K)
Shallow depth	$59.34 \times 10^5$	1739.64
Hemispherical	$69.19 \times 10^5$	1853.71
% increase	16.59	6.56

Table 2. Result comparison for emissions

Combustion chamber	Mass Fraction of Pollutant NO	Mass Fraction of Soot
Shallow Depth	$3.78 \times 10^{-07}$	$1.29 \times 10^{-13}$
Hemispherical	$4.26 \times 10^{-04}$	$2.53 \times 10^{-10}$

From the above compared results it had been found that hemispherical combustion chamber is producing more cylinder pressure and temperature. The percentage rise in pressure and temperature were also shown.

### 3.1 Carnot efficiency comparison

For Shallow depth combustion chamber:

$$\text{Carnot Efficiency} = (T_2 - T_1) / T_2$$

$$T_1 (\text{Initial temp}) = 750\text{K}$$

$$T_2 (\text{Final temp}) = 1739.64\text{K}$$

$$\begin{aligned} \text{Carnot Efficiency } (\eta) &= (1739.64 - 750) / 1739.64 \\ &= 0.569 \\ &= 56.9\% \end{aligned}$$

For Hemispherical combustion chamber

$$\text{Carnot Efficiency} = (T_2 - T_1) / T_2$$

$$T_1 (\text{Initial temp}) = 750\text{K}$$

$$T_2 (\text{Final temp}) = 1853.71\text{K}$$

$$\begin{aligned} \text{Carnot Efficiency } (\eta) &= (1853.71 - 750) / 1853.71 \\ &= 0.595 \\ &= 59.5\% \end{aligned}$$

$$\begin{aligned} \% \text{ increase in Carnot efficiency} &= \\ &= \{(59.5 / 56.9) * 100\} - 100 \\ &= 4.57\% \end{aligned}$$

### VII. CONCLUSION

The two combustion chamber models were modeled using ANSYS WORKBENCH and the combustion phenomena were analyzed using ANSYS FLUENT 14.5. The results show values comparable to theoretical values. Here two combustion chambers results were compared and following observations were made. The results are as follows:

- Numerical analysis result shows that hemispherical piston head provides much better performance than the shallow depth. This is due to the high turbulent intensity formed within the cylinder.
- Hemispherical combustion chamber is giving high pressure when compared to shallow depth combustion chamber. The pressure rise is about 16.59%.
- Hemispherical combustion chamber gives high temperature compared to shallow depth combustion chamber. The temperature rise is about 6.56%.
- When Carnot efficiency of both of the combustion chambers were compared it has been observed that carnot efficiency is more for hemispherical combustion chamber. When the increase in carnot efficiency is calculated, it is about 4.57%.
- The rise in temperature in hemispherical combustion chamber has shown significant increase of  $\text{NO}_x$  emissions and soot formation. In the combustion chambers  $\text{NO}_x$  emissions are

found at the regions of high temperature whereas soot formation is occurring at regions where temperature is comparatively low.

- NO<sub>x</sub> emissions can be reduced by changing injection timing as well as injection quantity.
- The change in geometry of combustion chambers that is by changing the piston head configurations considerable changes have been obtained.

#### REFERENCES

- [1] Apparao K, Srinivasa Rao P and Rajagopal K, "Study of multiple injections in (Homogeneous charge compression ignition) HCCI engine using computational fluid dynamics", Journal of Mechanical Engineering Research Vol. 3(4), pp. 103-113, April 2011.
- [2] A. R. Binesh, and S. Hossainpour, "Three Dimensional Modeling of Mixture Formation and Combustion in a Direct Injection Heavy-Duty Diesel Engine" , International Journal of Aerospace and Mechanical Engineering 2:4 2008.
- [3] Heywood, John B , "Internal combustion engines fundamentals", 1988, pp:668-671.
- [4] Joon Kyu Lee, Yong-Mo Kim, Jae-Hyun Ahn, "Numerical Modeling of Combustion Processes and Pollutants Formations in Direct-Injection Diesel Engines", KSME International Journal, VoL 16No. 7, pp. 1009--1018, 2002.
- [5] Mohamed Bencherif, Mohand Tazerout, Abdelkrim Liazid, "Turbulence-Combustion Interaction in Direct Injection Diesel Engine".
- [6] P.A. Lakshminarayanan ,Yogesh V. Aghav, " Modelling Diesel Combustion" ,Springer Publications, June 2009 , 09-281.
- [7] R. Manimaran, R. Thundil Karuppa Raj, K. Senthil Kumar, "Premixed Charge Compression Ignition in a Direct Injection Diesel Engine using Computational Fluid Dynamics".
- [8] Sudhakar Das, "CFD Study of Multiple Injections in a Diesel Engine" ILASS Americas, 25th Annual Conference on Liquid Atomization and Spray Systems, Pittsburgh, PA, May 2013.
- [9] Shahrir Abdullah, Wendy Hardyono Kurniawan and Azhari Shamsudeen, "Numerical Analysis of the Combustion Process in a Compressed Natural Gas Direct Injection Engine" Journal of Applied Fluid Mechanics, Vol. 1, No. 2, pp. 65-86, 2008.
- [10] Tutorial: *Modeling Non-Premixed Combustion*, "14.1 Description of the Equilibrium Mixture Fraction/ PDF Model , Fluent Inc. November 28, 2001".
- [11] Umakant V. Kongre , Vivek K. Sunnapwar, "CFD Modeling and Experimental Validation of Combustion in Direct Ignition Engine Fueled with Diesel", International Journal of Applied Engineering Research, Dindigul, Volume 1, no 3, 2010.
- [12] Watanabe T., Daidoji S., Keshav S. V, 2000, "Relationship between visible spray observations and DI diesel engine performance". Transaction of the ASME, vol.122,596-602.